

# Torsional waves in lossy cylinders

J. M. Carcione<sup>a)</sup> and G. Seriani<sup>b)</sup>

Osservatorio Geofisico Sperimentale, P.O. Box 2011 Opicina, 34016 Trieste, Italy

(Received 17 April 1997; revised 3 September 1997; accepted 10 October 1997)

The pure shear problem is one of relative mathematical simplicity and includes the essential physics common to more complicated cases, where multiple and coupled deformations occur. In this sense, the analysis of torsional waves serves as a pilot problem for investigating the influence of anisotropy and/or anelasticity on solution behavior. We obtain the kinematic and dynamic properties of torsional axially symmetric harmonic waves propagating in an infinitely long circular cylinder. The medium is transversely isotropic and dissipative, with its symmetry axis coincident with the axial axis of the cylinder. For an elastic cylinder each mode has a cutoff frequency and below that frequency there is no propagation. For tubes made of quartz and aluminum Lucite, we found that the existence of the cutoff frequencies depend on the degree of anisotropic attenuation, i.e., if the axial quality factor is greater than the transverse quality factor, the modes propagate at all frequencies. In contrast to the elastic case, the Poynting vector and the energy velocity have a component along the radial direction, whose values depend on the transverse attenuation. The presence of intrinsic attenuation confines the energy near the (elastic) cutoff frequencies while the radial distribution of the energy is governed by the geometrical features of the cylinder. © 1998 Acoustical Society of America. [S0001-4966(98)02002-5]

PACS numbers: 43.20.Jr, 43.20.Ks [JEG]

## INTRODUCTION

Laboratory measurements of wave propagation in cylindrical samples provide a method for estimating the elastic and anelastic properties of rocks and metals. For instance, intrinsic attenuation can be obtained from measurements in cylindrical bars (Kolsky, 1953; White, 1965; Blair, 1990; Tang, 1992). Moreover, analysis of wave propagation through hollow cylinders and tubes has many engineering applications (Soldatos, 1994), ranging from nondestructive evaluation of oil and gas pipelines, acoustic telemetry (Drumheller, 1993) to attenuation of waves inside rigid pipes containing acoustic liners (Greenspon and Singer, 1995). In the exploration industry, the interest resides in the propagation of pulses through drill strings, since these pulses are used as pilot signals for the data processing of seismograms generated by the roller cone bit (Rector and Hardage, 1992).

In this work, we compute the phase and energy velocities of torsional oscillations propagating in a lossy anisotropic hollow cylinder. The theory is a generalization of previous works (Mirsky, 1965a, b; Armenakas and Reitz, 1973; Carcione and Seriani, 1994) where a purely elastic cylinder was assumed.

## I. THE GOVERNING EQUATIONS

The problem is solved in cylindrical coordinates  $(r, \varphi, z)$  and an axially symmetric hollow cylinder of interior and exterior radii  $a$  and  $b$  is assumed. This implies that the symmetry axis of the medium coincides with the axial axis of the cylinder ( $z$  axis). In this case, the wave field does not depend on the azimuthal variable  $\varphi$ .

In absence of body forces, the equations describing the motion of torsional viscoelastic waves are

$$\rho \ddot{u}_\varphi = \partial_r \sigma_{\varphi r} + \partial_z \sigma_{\varphi z} + \frac{2}{r} \sigma_{\varphi r}, \quad (1)$$

$$\sigma_{\varphi r} = \dot{\psi}_{66} * \left( \partial_r u_\varphi - \frac{u_\varphi}{r} \right), \quad (2)$$

$$\sigma_{\varphi z} = \dot{\psi}_{44} * \partial_z u_\varphi, \quad (3)$$

where  $u_\varphi$  is the displacement component,  $\sigma_{\varphi r}$  and  $\sigma_{\varphi z}$  are the stress components,  $\rho$  is the density, and  $\psi_{44}$  and  $\psi_{66}$  are (time-dependent) relaxation functions. The symbol \* denotes time convolution,  $\partial$  spatial differentiation, and a dot above a variable time differentiation.

Since the torsional waves are decoupled from the quasi-compressional and quasi-shear motions, they can be described, as in the isotropic case, by a potential function  $\phi$ ,

$$u_\varphi = -\partial_r \phi. \quad (4)$$

Substituting the stresses into the conservation equation (1), and using Eq. (4), we obtain the equation of motion,

$$\rho \ddot{\phi} = \dot{\psi}_{44} * \partial_{zz} \phi + \dot{\psi}_{66} * \left( \partial_{rr} \phi + \frac{1}{r} \partial_r \phi \right). \quad (5)$$

## II. THE SOLUTION

The time-harmonic solution has the form

$$\phi = F(r, z) \exp(i\omega t), \quad (6)$$

where  $\omega$  is the angular frequency and  $\iota = \sqrt{-1}$ . Substitution of Eq. (6) into Eq. (5) gives the generalized Helmholtz equation

<sup>a)</sup>Electronic mail: jcarcione@ogs.trieste.it

<sup>b)</sup>Electronic mail: gseriani@ogs.trieste.it

$$\frac{1}{\beta^2 r} \partial_r (r \partial_r F) + \partial_{zz} F + \frac{\omega^2}{V^2} F = 0, \quad (7)$$

where

$$\beta = \sqrt{\frac{p_{44}}{p_{66}}} \quad (8)$$

and

$$p_{44} = \mathcal{F}(\dot{\psi}_{44}), \quad p_{66} = \mathcal{F}(\dot{\psi}_{66}) \quad (9)$$

are the complex stiffnesses, with the operator  $\mathcal{F}$  denoting the time Fourier transform. Moreover,

$$V = \sqrt{\frac{p_{44}}{\rho}} \quad (10)$$

is the complex body wave velocity along the symmetry axis of the medium.

The general solution for time-harmonic waves along the positive  $z$  direction is

$$\begin{aligned} \phi(r, z, t; \gamma, \omega) = & [A_0 J_0(kr) + B_0 Y_0(kr)] \\ & \times \exp[\iota(\omega t - \gamma z)], \end{aligned} \quad (11)$$

where  $J_0$  and  $Y_0$  are Bessel functions of the first and second kinds, respectively, and  $A_0$  and  $B_0$  are arbitrary constants. The radial and vertical wave numbers  $k$  and  $\gamma$  are related by

$$k^2 = \beta^2 \left( \frac{\omega^2}{V^2} - \gamma^2 \right). \quad (12)$$

Application of the boundary conditions at the inner and outer surfaces of the cylinder,

$$\sigma_{\varphi r}(r=a) = 0 \quad \text{and} \quad \sigma_{\varphi r}(r=b) = 0, \quad (13)$$

imply

$$A_0 J_2(ka) + B_0 Y_2(ka) = 0, \quad (14)$$

$$A_0 J_2(kb) + B_0 Y_2(kb) = 0, \quad (15)$$

where the following properties were used:  $\partial_r J_0(kr) = -kJ_1(kr)$  and  $(\partial_{rr} - r^{-1}\partial_r)J_0(kr) = k^2 J_2(kr)$ . Making zero the determinant of the linear system gives the period or dispersion equation

$$J_2(ka)Y_2(kb) - J_2(kb)Y_2(ka) = 0. \quad (16)$$

Equation (16) is identical to the purely elastic period dispersion, where the roots  $k_1, k_2, \dots, k_j, \dots$  are real. Abramowitz and Stegun (1964, p. 374) give an approximate formula for the root  $q_j \equiv k_j a$  that can be used for  $b/a < 3$ . Here, we compute the exact roots by using the Mathematica software.

The velocity of the lowest torsional mode is not appropriately obtained from Eq. (16). This mode corresponds to  $k=0$  and the displacement to a rotation of each transverse section of the cylinder as a whole about its center [see, for instance, Christensen (1982), p. 47]. The dispersion of this mode is caused by the intrinsic attenuation along the radial direction. The phase velocity is

$$c_p = [\text{Re}(V^{-1})]^{-1}, \quad (17)$$

where  $\text{Re}$  denotes the real part.

### III. PHYSICAL VELOCITIES AND DISSIPATION FACTORS

The location of a pulse traveling in the axial direction requires the explicit calculation of the energy velocity, since the concept of group velocity loses its physical meaning. The presence of attenuation considerably distorts the modulation envelope of the pulse (e.g., Carcione, 1994). Besides the presence of intrinsic attenuation, the energy velocity displays local information not contained in the group velocity (see the discussion in Simmons *et al.*, 1992).

#### A. Phase velocity and attenuation factor

The phase velocity and attenuation factor versus frequency corresponding to the  $j$  mode are

$$c_p(\omega) = \frac{\omega}{\text{Re}(\gamma)} \quad \text{and} \quad \alpha(\omega) = -\text{Im}(\gamma), \quad (18)$$

where

$$\gamma(\omega) = \frac{\omega}{c_p} - \iota\alpha = \text{p.v.} \left( \frac{\omega^2}{V^2(\omega)} - \frac{k_j^2}{\beta^2(\omega)} \right)^{1/2}, \quad (19)$$

with p.v. denoting the principal value and  $\text{Im}$  the imaginary part.

The calculation of the phase velocity and attenuation versus wavelength is not straightforward. Since

$$\lambda(\omega) \equiv G(\omega) = \frac{2\pi}{\text{Re}[\gamma(\omega)]}, \quad (20)$$

$\omega = G^{-1}(\lambda)$  and a formal solution is

$$c_p(\lambda) = \frac{\lambda}{2\pi} G^{-1}(\lambda) \quad \text{and} \quad \alpha = \text{Im}\{\gamma[G^{-1}(\lambda)]\}. \quad (21)$$

However, relation (20) is, in general, not invertible. The most simple procedure is to plot the pairs  $[c_p(\omega), \lambda(\omega)]$  and  $[\alpha(\omega), \lambda(\omega)]$ .

#### B. Energy velocity and quality factor

Calculation of the energy velocity and quality factor requires energy considerations. The Umov–Poynting theorem, or energy balance equation, for time-harmonic fields in anisotropic-viscoelastic media (Carcione and Cavallini, 1993) is

$$\text{div } \mathbf{P} - 2\iota\omega(\langle \epsilon_s \rangle - \langle \epsilon_v \rangle) + \omega \langle \epsilon_d \rangle = 0, \quad (22)$$

where  $\mathbf{P}$  is the complex Umov–Poynting vector defined as

$$\mathbf{P} = -\frac{1}{2} \boldsymbol{\Sigma} \cdot \dot{\mathbf{u}}^*, \quad (23)$$

with  $\boldsymbol{\Sigma}$  the stress tensor,

$$\langle \epsilon_v \rangle = \frac{1}{4} \rho \dot{\mathbf{u}}^T \cdot \dot{\mathbf{u}}^* \quad (24)$$

is the time-average kinetic energy density,

$$\langle \epsilon_s \rangle = \text{Re}(\mathcal{E}) \quad \text{and} \quad \langle \epsilon_d \rangle = 2 \text{Im}(\mathcal{E}) \quad (25)$$

are the time-average stored and dissipated energy densities, respectively, with

$$\mathcal{E} = \frac{1}{4} \mathbf{S}^T \cdot \mathbf{p} \cdot \mathbf{S}^* \quad (26)$$

the complex energy density,  $\mathbf{S}$  the strain vector, and  $\mathbf{p}$  the complex stiffness matrix. The asterisk used as superscript denotes complex conjugation, the symbol  $\cdot$ , ordinary matrix multiplication, and the superscript  $\mathsf{T}$ , transpose.

The Poynting vector is

$$\mathbf{P} = -\frac{1}{2}(\sigma_{\varphi z}\hat{\mathbf{e}}_z + \sigma_{\varphi r}\hat{\mathbf{e}}_r)u_\varphi^* \quad (27)$$

Substituting the potential (11) into Eq. (4) and using Eq. (14) gives

$$u_\varphi = kA_0R_1 \exp(-\alpha z)\exp[\iota\omega(t-z/c_p)], \quad (28)$$

where

$$R_i(kr) = J_i(kr) - \frac{J_2(ka)}{Y_2(ka)} Y_i(kr), \quad i=1,2. \quad (29)$$

Note that  $R_2(ka)=0$  and by virtue of the dispersion equation (16),  $R_2(kb)=0$ . The stress components are given by Eqs. (2) and (3),

$$\sigma_{\varphi z} = -\iota\gamma k p_{44} A_0 R_1 \exp(-\alpha z)\exp[\iota\omega(t-z/c_p)], \quad (30)$$

$$\sigma_{\varphi r} = -k^2 p_{66} A_0 R_2 \exp(-\alpha z)\exp[\iota\omega(t-z/c_p)]. \quad (31)$$

Then,

$$\mathbf{P} = \frac{1}{2}\omega k^2 |A_0|^2 R_1 (p_{44}\gamma R_1 \hat{\mathbf{e}}_z - \iota p_{66} k R_2 \hat{\mathbf{e}}_r) \exp(-2\alpha z). \quad (32)$$

From Eq. (26), the complex energy density is

$$\mathcal{E} = \frac{1}{4}(p_{44}|S_{\varphi z}|^2 + p_{66}|S_{\varphi r}|^2), \quad (33)$$

where

$$S_{\varphi z} = \partial_z u_\varphi \quad \text{and} \quad S_{\varphi r} = \partial_r u_\varphi - \frac{u_\varphi}{r} \quad (34)$$

are the strain components. Using Eq. (28) we obtain

$$\mathcal{E} = \frac{1}{4}k^2 |A_0|^2 (p_{44}|\gamma|^2 R_1^2 + p_{66}k^2 R_2^2) \exp(-2\alpha z). \quad (35)$$

The kinetic energy density is simply

$$\langle \epsilon_v \rangle = \frac{1}{4}\rho\omega^2 k^2 |A_0|^2 R_1^2 \exp(-2\alpha z). \quad (36)$$

In contrast to unbounded homogeneous and elastic media, the average kinetic and potential energy densities are different in elastic cylinders. This is shown in the Appendix.

The energy velocity  $\mathbf{v}_e$  is the ratio of the average power flow density  $\text{Re}(\mathbf{P})$  to the mean energy density  $\langle \epsilon_v + \epsilon_s \rangle$ . Then,

$$\begin{aligned} \mathbf{v}_e &= \frac{\text{Re}(\mathbf{P})}{\langle \epsilon_v + \epsilon_s \rangle} \\ &= \frac{2\omega[\text{Re}(\gamma p_{44})R_1^2 \hat{\mathbf{e}}_z + k \text{Im}(p_{66})R_1 R_2 \hat{\mathbf{e}}_r]}{\rho\omega^2 R_1^2 + |\gamma|^2 R_1^2 \text{Re}(p_{44}) + k^2 R_2^2 \text{Re}(p_{66})}. \end{aligned} \quad (37)$$

Equation (37) becomes

$$\mathbf{v}_e = \frac{2\omega[\text{Re}(\gamma p_{44})\hat{\mathbf{e}}_z + k \text{Im}(p_{66})(R_2/R_1)\hat{\mathbf{e}}_r]}{\rho\omega^2 + |\gamma|^2 \text{Re}(p_{44}) + k^2 \text{Re}(p_{66})(R_2/R_1)^2}. \quad (38)$$

Note that the dependence on the radial variable  $r$  is contained in  $R_2/R_1$ . While the energy velocity is constant for a plane wave in unbounded media, it is a function of  $r$  for

cylindrical systems and has a component in the radial direction. This component vanishes in the purely elastic case, since  $\text{Im}(p_{66})=0$ . At  $r=a$  and  $r=b$ ,  $R_2$  vanishes and using Eq. (10),

$$\mathbf{v}_e = \frac{2\omega \text{Re}(\gamma V^2)}{\omega^2 + |\gamma|^2 \text{Re}(V^2)} \hat{\mathbf{e}}_z. \quad (39)$$

The quality factor can be obtained as the ratio of twice the stored energy to the dissipated energy, giving

$$Q = \frac{2\langle \epsilon_s \rangle}{\langle \epsilon_d \rangle} = \frac{\text{Re}(p_{44})|\gamma|^2 + k^2 \text{Re}(p_{66})(R_2/R_1)^2}{\text{Im}(p_{44})|\gamma|^2 + k^2 \text{Im}(p_{66})(R_2/R_1)^2}. \quad (40)$$

At  $r=a$  and  $r=b$  Eq. (40) reduces to

$$Q = \frac{\text{Re}(p_{44})}{\text{Im}(p_{44})}, \quad (41)$$

that is, the quality factor of the shear body wave traveling along the symmetry axis of the medium.

#### IV. EXAMPLES

We use a phenomenological model based on a viscoelastic rheology. The theory assumes a single standard linear solid element describing the anelastic deformations associated with the axial direction ( $\nu=1$ ) and the radial direction ( $\nu=2$ ). We take

$$p_{44} = c_{44}M_1, \quad p_{66} = c_{66}M_2, \quad (42)$$

where the complex moduli can be expressed as

$$M_\nu(\omega) = \frac{\sqrt{Q_{0\nu}^2 + 1} - 1 + i\omega Q_{0\nu}\tau_0}{\sqrt{Q_{0\nu}^2 + 1} + 1 + i\omega Q_{0\nu}\tau_0}. \quad (43)$$

The quality factor  $Q_\nu$ , associated with of each moduli, is equal to the real part of  $M_\nu$  divided by its imaginary part. The curve  $Q_\nu^{-1}(\omega)$  has its peak at  $\omega_0 = 1/\tau_0$ , and the value of  $Q_\nu$  at the peak is  $Q_{0\nu}$ . The high-frequency limit corresponds to the elastic case with  $M_\nu \rightarrow 1$ . The relaxation functions associated with the complex stiffnesses are  $\psi_{44} = c_{44}\chi_1$  and  $\psi_{66} = c_{66}\chi_2$ , where

$$\chi_\nu(t) = \left[ \frac{\tau_+^{(\nu)}}{\tau_-^{(\nu)}} - \left( \frac{\tau_-^{(\nu)}}{\tau_+^{(\nu)}} - 1 \right) \exp(-t/\tau_+^{(\nu)}) \right] H(t), \quad (44)$$

with  $H(t)$  the Heaviside function, and

$$\tau_\pm^{(\nu)} = \frac{\tau_0}{Q_{0\nu}} [\sqrt{Q_{0\nu}^2 + 1} \pm 1]. \quad (45)$$

We introduce the anisotropic loss parameter

$$\eta = \frac{Q_{01}}{Q_{02}} \quad (46)$$

and assume that  $\eta = 1.2\beta_\infty$ , where  $\beta_\infty = \beta(\omega \rightarrow \infty) = \sqrt{c_{44}/c_{66}}$ .

We consider two materials (see Thomsen, 1986); quartz, with  $c_{44} = 53.21$  GPa,  $\rho = 2.65$  gr/cm<sup>3</sup>,  $\beta_\infty = 1.21$  and  $Q_{01} = 100$ ; and aluminum-Lucite composite with  $c_{44} = 3.4$  GPa,  $\rho = 1.86$  gr/cm<sup>3</sup>,  $\beta_\infty = 0.53$  and  $Q_{01} = 10$ . The calculations are carried out for samples having  $a = 1$  cm and  $b = 2$  cm. If  $q_j$

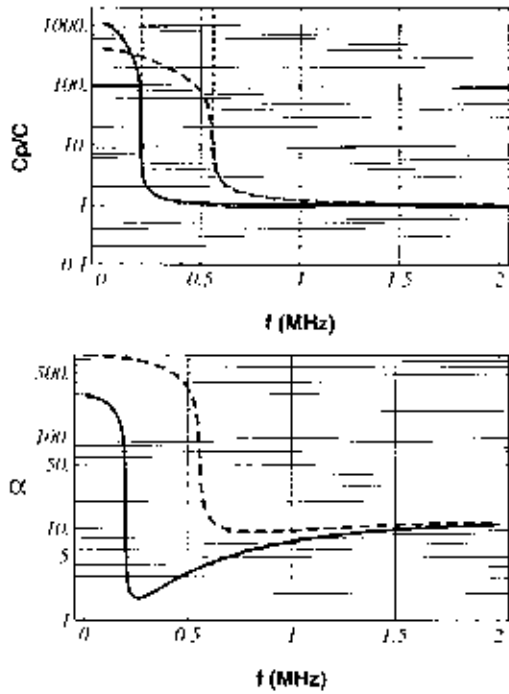


FIG. 1. Quartz: normalized phase velocity and attenuation versus frequency corresponding to the first and third propagation modes (continuous and broken lines, respectively). The normalization constant is the axial elastic velocity  $c = (c_{44}/\rho)^{1/2}$ . The thin broken lines are the respective elastic phase velocities.

$=k_j a$ , the first three roots of the dispersion equation (16) are  $q_1 = 3.4069$ ,  $q_2 = 6.4278$ , and  $q_3 = 9.5228$ . These roots are independent of the material properties.

### A. Quartz

Normalized phase velocity and attenuation versus frequency corresponding to the first and third propagation modes are represented in Fig. 1 (continuous and broken lines, respectively). The thin broken lines are the respective elastic phase velocities, that tend to infinity at the cutoff frequencies  $f_c = 201$  kHz and  $f_c = 561$  kHz [ $\gamma = 0$  in Eq. (12)]. There are no cutoff frequencies in the viscoelastic case, although the attenuations below  $f_c$  are so high that wave propagation is precluded in practice.

Figure 2 represents the normalized displacement field (32) for mode 3 as a function of frequency and radial distance (from  $r = a$  to  $r = b$ ). The upper picture corresponds to  $z = 0$  and the lower picture to  $z = 0.1$  m. In this case, the strong attenuation below the (elastic) cutoff frequency prevents any particle motion. Moreover, the viscoelasticity causes the dissipation at high frequencies.

The modulus of the normalized energy velocity, versus frequency and radial distance, is represented in Fig. 3. The surface practically shows the axial component of the energy velocity vector, since the radial component is very small. The energy velocity vanishes where there is no particle motion (see Fig. 2). These minima in the energy velocity are not due to the elasticity but to the geometrical features of the cylinder. As can be seen, the energy velocity displays local information not contained in the group velocity. It can be shown that the elastic energy velocity, when defined as the

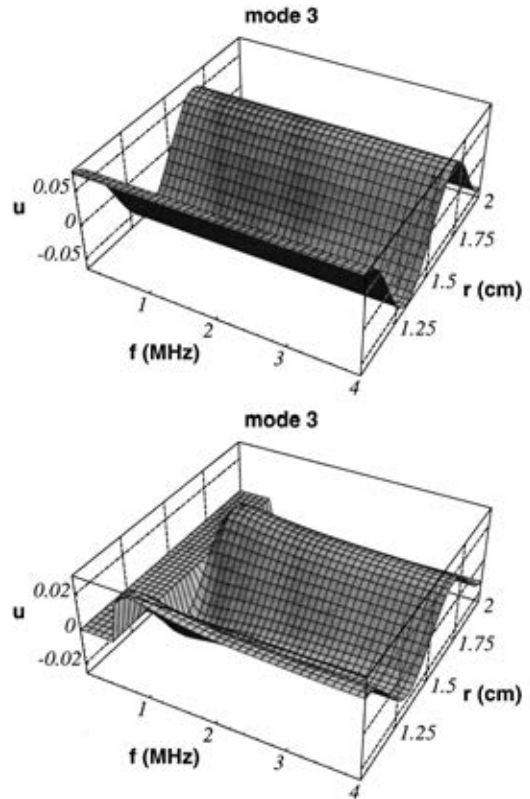


FIG. 2. Quartz: normalized displacement field for mode 3 as a function of frequency and radial distance. The upper picture corresponds to  $z = 0$  and the lower picture to  $z = 0.1$  m. The normalization constant is the displacement at  $f = 1$  MHz,  $r = a$  and  $z = 0$ .

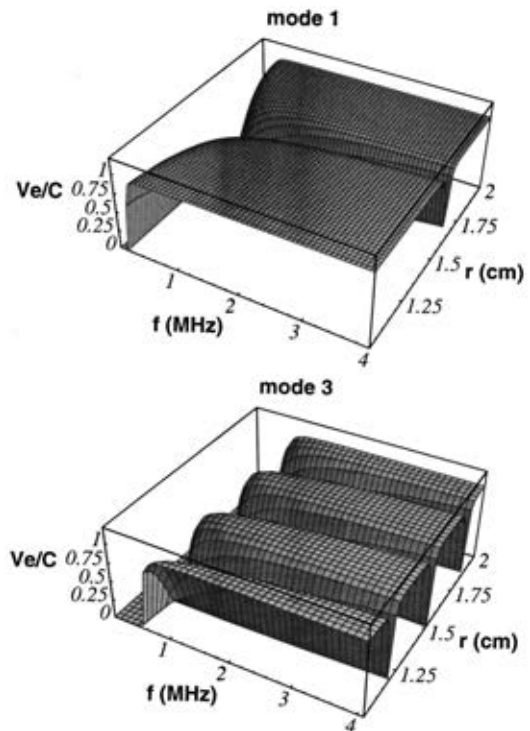


FIG. 3. Quartz: modulus of the normalized energy velocity, versus frequency and radial distance. The normalization constant is the axial elastic velocity  $c = (c_{44}/\rho)^{1/2}$ .

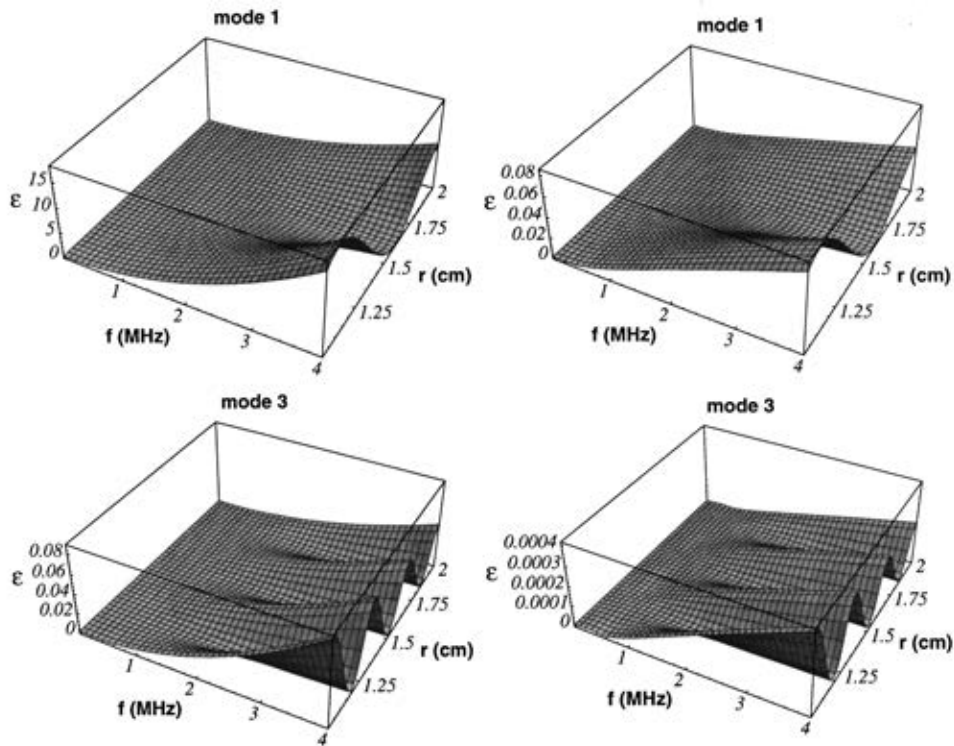


FIG. 4. Quartz: distribution of the energy along the radial distance, as a function of frequency. The left pictures correspond to the mean energy density  $\langle \epsilon_v + \epsilon_s \rangle$  and the right pictures are the dissipated energy densities  $\langle \epsilon_d \rangle$ . The normalization constant  $\epsilon_0$  is the total energy at  $f=1$  MHz,  $r=a$  and  $z=0$ .

ratio of the time average of the power per cross section and the time average of the total energy per unit length of cylinder, equals the group velocity (e.g., Achenbach, 1973, pp. 214).

Figure 4 shows the distribution of the energy along the radial distance, as a function of frequency. The left pictures correspond to the mean energy density  $\langle \epsilon_v + \epsilon_s \rangle$  and the right pictures are the dissipated energy densities  $\langle \epsilon_d \rangle$ . The first

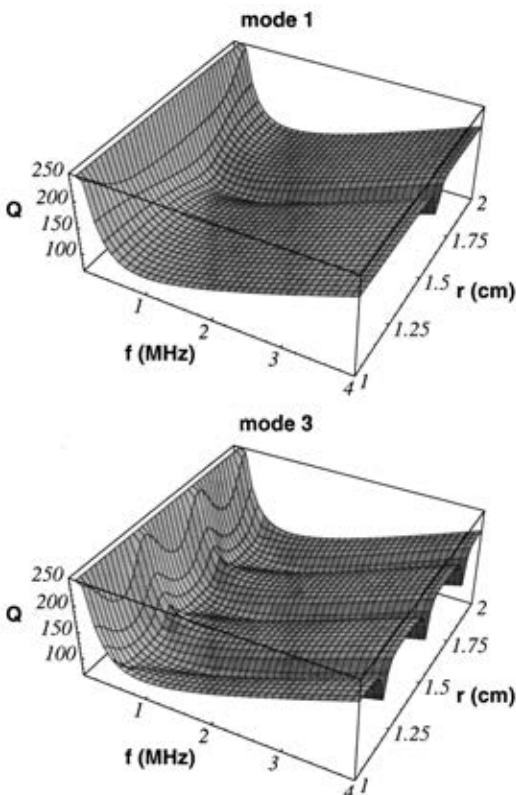


FIG. 5. Quartz: quality factors versus frequency and radial distance.

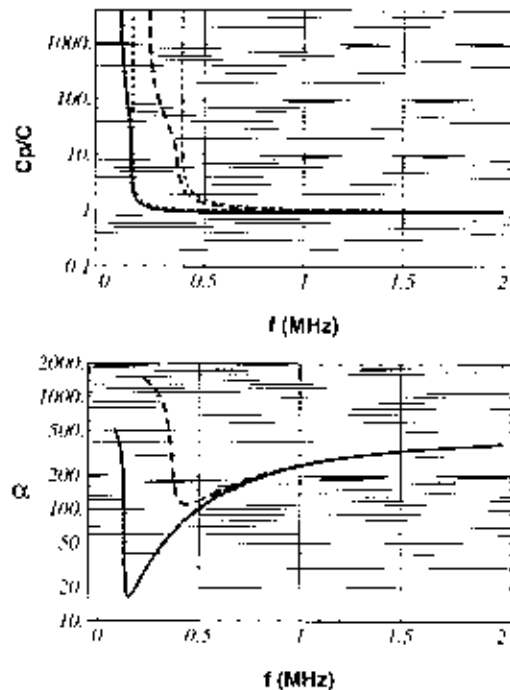


FIG. 6. Aluminum Lucite: phase velocity and attenuation curves versus frequency, corresponding to the first and third propagation modes (continuous and broken lines, respectively). The normalization constant is the axial elastic velocity  $c = (c_{44}/\rho)^{1/2}$ . The thin broken lines are the respective elastic phase velocities.

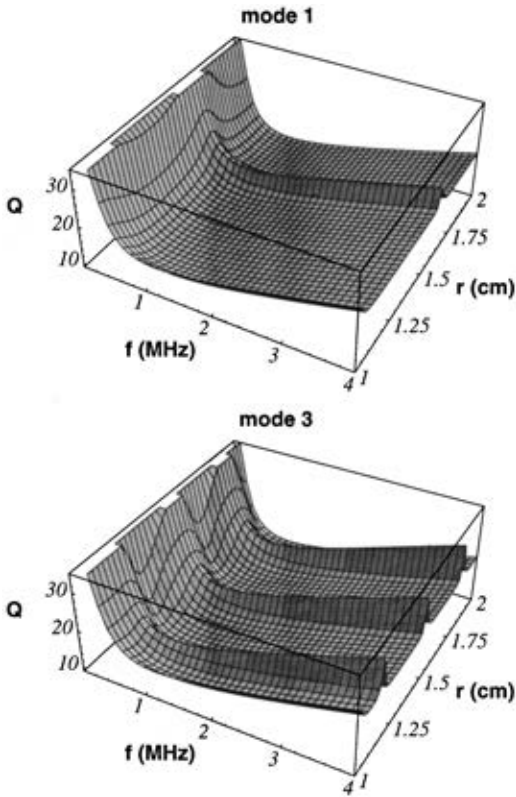


FIG. 7. Aluminum Lucite: quality factors versus frequency and radial distance.

mode is approximately 200 times stronger than the third mode, and both modes carry more energy at the high frequencies. This happens at the onset of the perturbation ( $z = 0$ ), since for  $z \neq 0$  the high frequencies are attenuated by the viscoelastic effects and the motion is confined near the (elastic) cutoff frequencies (Fig. 2).

Finally, the quality factors are represented in Fig. 5. They have a minimum value at  $\omega_0$ , the location of the relaxation peak. The location of the minima along the radial direction coincide with the positions of zero particle motion (see Fig. 2).

It is important to distinguish between two attenuation effects. One is of viscoelastic nature, that is reflected in the shape of the quality factors surface as a function of frequency. The other is geometrical effect that produce the minima along the radial direction and causes the strong attenuation below the elastic cutoff frequencies (see Fig. 1).

## B. Aluminum Lucite

In contrast to quartz, this material has  $\eta < 1$ , and therefore, the attenuation is higher along the axial direction. Due to this fact, the physics of wave propagation is different. Figure 6 shows the phase velocity and attenuation curves versus frequency. In this case, there is a cutoff frequency even in the presence of anelasticity. The displacements energy densities and energy velocity surfaces are similar to those of quartz. The quality factors are represented in Fig. 7. They have a minimum value at  $\omega_0$ , the location of the relaxation peak, and, unlike quartz, the surfaces presents maxima along the radial direction.

## APPENDIX: ENERGY BALANCE

In unbounded media  $\text{div } \mathbf{P} = -2\alpha \cdot \mathbf{P}$  (Carcione and Cavallini, 1993). If there are no losses, Eq. (22) implies that the average kinetic energy equals the average potential energy. An analysis based on Eq. (22) shows that this is not the case for cylinders. In order to verify the energy balance Eq. (22) we explicitly calculate the divergence of the Poynting vector (32). This can be written as

$$\mathbf{P} = P_r \hat{\mathbf{e}}_r + P_z \hat{\mathbf{e}}_z, \quad (\text{A1})$$

where

$$P_r = p_r R_1 R_2 \exp(-2\alpha z), \quad p_r = -\frac{i}{2} \omega k^3 |A_0|^2 p_{66} \quad (\text{A2})$$

and

$$P_z = p_z R_1^2 \exp(-2\alpha z), \quad p_z = \frac{1}{2} \omega k^2 |A_0|^2 \gamma p_{44}. \quad (\text{A3})$$

We have that

$$\text{div } \mathbf{P} = \partial_r P_r + \frac{P_r}{r} + \partial_z P_z. \quad (\text{A4})$$

For computing the radial derivatives we use the following recurrence relation for the cylinder functions  $\mathcal{C}(z)$ , where  $z$  is complex and  $\nu$  any number (not necessarily an integer):

$$z \mathcal{C}'_\nu = \nu \mathcal{C}_\nu - z \mathcal{C}_{\nu+1} = -\nu \mathcal{C} + z \mathcal{C}_{\nu-1}. \quad (\text{A5})$$

We obtain

$$\partial_r P_r = p_r k \left( R_1^2 - R_2^2 - \frac{1}{r} R_1 R_2 \right) \exp(-2\alpha z). \quad (\text{A6})$$

Then,

$$\text{div } \mathbf{P} = [(k p_r - 2\alpha p_z) R_1^2 - k p_r R_2^2] \exp(-2\alpha z). \quad (\text{A7})$$

Note that in the elastic case the kinetic energy is not equal to the potential energy (in average), since

$$\langle \epsilon_s \rangle - \langle \epsilon_v \rangle = -\frac{1}{4} k^4 |A_0|^2 c_{66} (R_1^2 - R_2^2). \quad (\text{A8})$$

However, using properties of the cylinder functions, it can be shown that

$$\int [R_1^2(kr) - R_2^2(kr)] r dr = kr R_1(kr) R_2(kr), \quad (\text{A9})$$

Then, integration of Eq. (A8) over the cross section of the cylinder is zero since  $R_2(ka) = 0$  and  $R_2(kb) = 0$ . This is in agreement with the result obtained by Achenbach (1973, pp. 214).

- Abramowitz, M., and Stegun, I. A., Eds. (1964). *Handbook of Mathematical Functions*, Applied Mathematical Series 55, p. 374, National Bureau of Standards, Washington, D. C.
- Achenbach, J. D. (1973). *Wave Propagation in Elastic Solids* (North-Holland, Amsterdam).
- Armenakas, A., and Reitz, E. S. (1973). "Propagation of harmonic waves in orthotropic circular cylindrical shells," *J. Appl. Mech.* **30**, 168–174.
- Blair, D. P. (1990). "The longitudinal pulse velocity in finite cylindrical cores," *J. Acoust. Soc. Am.* **88**, 1123–1131.
- Carcione, J. M. (1994). "Wavefronts in dissipative anisotropic media," *Geophysics* **59**, 644–657.
- Carcione, J. M., and Cavallini, F. (1993). "Energy balance and fundamental relations in anisotropic viscoelastic media," *Wave Motion* **18**, 11–20.
- Carcione, J. M., and Seriani, G. (1994). "Torsional oscillations of anisotropic hollow circular cylinders," *Acoust. Lett.* **18**, 99–102.
- Christensen, R. M. (1982). *Theory of Viscoelasticity. An Introduction* (Academic, New York).
- Drumheller, D. S. (1993). "Attenuation of sound waves in drill strings," *J. Acoust. Soc. Am.* **94**, 2387–2396.
- Greenspan, J. E., and Singer, E. G. (1995). "Propagation in fluids inside thick viscoelastic cylinders," *J. Acoust. Soc. Am.* **97**, 3502–3509.
- Kolsky, H. (1953). *Stress Waves in Solids* (Clarendon, Oxford), pp. 136–141.
- Mirsky, I. (1965a). "Wave propagation in transversely isotropic hollow circular cylinders, Part I: Theory," *J. Acoust. Soc. Am.* **37**, 1016–1021.
- Mirsky, I. (1965b). "Wave propagation in transversely isotropic hollow circular cylinders, Part II: Numerical results," *J. Acoust. Soc. Am.* **37**, 1022–1026.
- Rector III, J. W., and Hardage, B. A. (1992). "Radiation pattern and seismic waves generated by a working roller-cone drill bit," *Geophysics* **57**, 1319–1333.
- Simmons, J. A., Drescher-Krasicka, E., and Wadley, H. N. G. (1992). "Leaky axisymmetric modes in infinite clad rods," *J. Acoust. Soc. Am.* **92**, 1061–1090.
- Soldatos, K. P. (1994). "Review of three dimensional dynamic analyses of circular cylinders and cylindrical shells," *Appl. Mech. Rev.* **47**, 501–516.
- Tang, X. M. (1992). "A waveform inversion technique for measuring elastic wave attenuation in cylindrical bars," *Geophysics* **57**, 854–859.
- Thomsen, L. (1986). "Weak elastic anisotropy," *Geophysics* **51**, 1954–1966.
- White, J. E. (1965). *Seismic Waves, Radiation, Transmission and Attenuation* (McGraw-Hill, New York).